

# Molecular Hydrogen-rich Interstellar Ice

Richard W. Dissly<sup>1</sup>

Mark Allen<sup>1,2</sup>

Vincent Anicich<sup>2</sup>

<sup>1</sup>Division of Geological and Planetary Sciences, California Institute of Technology, MS 170-25, Pasadena, CA 91125

<sup>2</sup>Earth and Space Sciences Division, Jet Propulsion Laboratory, MS 183-601, California Institute of Technology, 4800 Oak Grove Drive, Pasadena, CA 91109

While molecular hydrogen is by far the most abundant gas phase molecule in interstellar dark clouds, the extreme volatility of  $H_2$  suggests that it has a relatively low abundance in grain volatile mantles, thought to be composed largely of amorphous water ice<sup>1, 2</sup>. Models of the chemistry on grain surfaces can be quite sensitive to surface structure and composition<sup>3</sup>. The expected composition of an average grain mantle is therefore a crucial part of understanding the contribution of surface reactions to interstellar chemistry. We have simulated the formation of interstellar water ice mantles in the presence of  $H_2$ , using thin film deposition and temperature programmed desorption. Our results show a high molar composition ratio of  $H_2/H_2O \approx 2$ , with a substantial population of the hydrogen stable in the ice above 40 K, suggesting that icy grain mantles are rich in  $H_2$ . The stability of  $H_2$  in water ice mantles is due to a distribution of binding site energies, as high as 1500 K. We speculate on the implications for grain mantle chemistry and physics.

Although molecular hydrogen is known to be produced catalytically on interstellar grain surfaces, the amount of recondensation of  $H_2$  onto grains is uncertain. Experimental results for the binding energy of  $H_2$  on a surface of amorphous water ice range from 360 K to 860 K<sup>4-6</sup>, with the binding energy gradually decreasing to  $\sim 100$  K (the sublimation energy of solid  $H_2$  ice) as the surface coverage of adsorbed  $H_2$  increases. Theoretical predictions of the amount of  $H_2$  on grain surfaces based on these disparate results vary accordingly, from a thick mantle of predominantly  $H_2$  ice that can strongly inhibit surface chemistry<sup>3</sup>, to a thin monolayer of  $H_2$  that has relatively little effect on the surface reactions of other species<sup>6-9</sup>. In the latter view, the subsequent accumulation of other species on top of the molecular hydrogen is ignored, so that  $H_2$  is only seen as a surface component. Recent work has shown that amorphous water ice at temperatures above 16K has the capacity to internally trap a large amount of hydrogen when codeposited<sup>10</sup>, suggesting that  $H_2$  may be a component throughout the volume of an icy grain mantle. In light of these issues, we have tried to experimentally determine the amount of  $H_2$  that can be incorporated in amorphous  $H_2O$  grain mantles under interstellar conditions.

Experimental work on the structure of vapor-deposited amorphous water indicates that the surface area of the ice is dependent on the deposition conditions<sup>11</sup>. We have tried to control our deposition parameters to simulate as closely as possible the formation of interstellar icy mantles, using an experimental arrangement similar to that described elsewhere<sup>12</sup>. The ice samples were prepared by simultaneously spraying  $H_2$  and  $H_2O$  from separate gas lines slowly onto a cooled sapphire window into a vacuum of a few  $\times 10^{-8}$  torr. The gases were sprayed from pinholes 0.06 mm in diameter, set 4.0 cm away from the window, with nozzle backing pressures of between 0.05 torr and 1.2 torr. This yields a Knudsen number (ratio of mean free path of gas in reservoir to nozzle diameter) for our deposition of between 1.2 and 12, i.e., in the molecular flow regime. This gives a microporous ice with high surface area<sup>11</sup>, as one would

expect for the slow growth of interstellar grain mantles. Transmittance spectra between 2000 and 5000  $\text{cm}^{-1}$  then were taken of the ice samples at a resolution  $\leq 1 \text{ cm}^{-1}$ .

Depositions were carried out for several window temperatures between 12 and 30 K, at a growth rate of approximately  $0.2 \mu\text{m/hr}$ . Once the deposition was completed, the sample was allowed to sit  $\sim 10$  minutes, until the pressure in the chamber had equilibrated. The sample was then heated (typically at a rate of 2 K/min), and the evolved gases were monitored with a quadrupole mass spectrometer, calibrated to the absolute partial pressures of both  $\text{H}_2$  and  $\text{H}_2\text{O}$ . We derived the rate of gas release from the sample, using the following formula:

$$\text{Desorption Rate}[\text{molec/minute}] = \text{Pumping speed}[\text{l/min}] * \text{Number density}[\text{molec/l}]$$

with the number density of each gas determined from the mass spectrometer reading, and pumping speeds (100 l/s for  $\text{H}_2\text{O}$ , and 66 l/s for  $\text{H}_2$ ) determined by the pump manufacturer. Integrating this rate over the time it takes for the entire ice sample to sublimate gives the total abundance of  $\text{H}_2$  and  $\text{H}_2\text{O}$  in the sample.

To assure that the relative gas collision rate of  $\text{H}_2$  with the growing ice was greater than that of  $\text{H}_2\text{O}$ , the samples were prepared with relative gaseous  $\text{H}_2:\text{H}_2\text{O}$  inlet pressures of between 4:1 and 36:1; deposition times ranged between 20 minutes and 2.5 hours. As shown in figure 1, the amount of  $\text{H}_2$  released upon heating the sample correlates with the amount of  $\text{H}_2\text{O}$  present. The  $\text{H}_2/\text{H}_2\text{O}$  ratio in our ice samples did not depend on the input ratio in any systematic way, suggesting that the maximum amount of hydrogen that can be incorporated is quickly reached for a small excess of  $\text{H}_2$  over  $\text{H}_2\text{O}$ . Spraying only  $\text{H}_2$  onto the 12 K window yielded very little hydrogen upon heating, indicating that  $\text{H}_2\text{O}$  ice is the substrate responsible for the  $\text{H}_2$  binding. In all the mixed  $\text{H}_2/\text{H}_2\text{O}$  ice depositions, hydrogen was the primary component, with the  $\text{H}_2/\text{H}_2\text{O}$  relative composition in the range of 1.6 to 3.7 (average value of  $\sim 2$ ), significantly higher than previous results<sup>10, 13</sup>.

The temperature programmed desorption profiles for both  $\text{H}_2$  and  $\text{H}_2\text{O}$  are shown in figure 2, for depositions at different window temperatures. The relative amount of hydrogen in the water ice decreases significantly as the substrate temperature increases, with  $\text{H}_2/\text{H}_2\text{O}$  ratios of 1.6, 0.5, and  $\leq 0.1$  for the depositions at 12 K, 20 K, and 30 K, respectively. From the 12 K deposition in particular, it is apparent that, while most of the  $\text{H}_2$  sublimates below 30 K, a significant population of strongly bound  $\text{H}_2$  exists in the water ice, released as high as 70 K.

To prove that this high temperature component was not simply due to the time-delayed diffusion of unbound hydrogen from deeper layers in the ice, we performed the stepwise heating experiment shown in figure 3. The temperature of this ice sample was held constant for  $\sim 10$  minutes at several points during the

heating process, to allow for the complete release of any labile  $H_2$  in the sample volume. During the temperature holds, the  $H_2$  release rate dropped quickly to the background level. When we resumed increasing sample temperature, the  $H_2$  release rate returned to the value when the increase in temperature was halted. These results suggest that the release of  $H_2$  at temperatures up to 70 K reflects the spectrum of binding site energies in the volume of the  $H_2/H_2O$  ice sample, rather than a possible diffusive delay for hydrogen escape. The respective integrated flux for each temperature interval then represents the relative amount of  $H_2$  stable in that interval: for  $T \leq 20$  K, 63%; 20-30 K, 18%; 30-40 K, 4%; and  $T > 40$  K, 15%. The corresponding binding site energies ( $E_b$ , in units of Kelvin) can be determined by assuming that the  $H_2$  was released from the sample at temperature  $T$  when the sublimation timescale ( $\tau_{sub}$ ) was equal to the sampling timescale in the experiment,  $\sim 10^3$  sec. Then values for  $E_b$  can be derived from the expression,  $\tau_{sub} \approx \tau_{vib} \exp[E_b/kT]$ , where  $\tau_{vib} \approx 10^{-13}$  sec, a characteristic vibrational period. Between 12-20 K,  $H_2$  sublimated from sites with  $E_b \approx 440$  K-740 K, and between 20-30 K, 30-40 K, and  $> 40$  K, from sites with  $E_b \approx 740$  K-1100 K, 1100 K-1475 K, and  $\geq 1475$  K, respectively. Because of the delay of  $\sim 10$  minutes between the end of the deposition and the beginning of the measured desorption, hydrogen in sites of  $E_b \leq 440$  K sublimated before measurements were started. That the largest number of sites had  $E_b \leq 740$  K, with a decreasing number out to  $\sim 2000$  K, agrees qualitatively with theoretical estimates for the distribution of  $H_2$  binding sites in amorphous  $H_2O$  ice<sup>13</sup>, with the exception of the secondary peak at the highest energies which we attribute to sites located deep in the ice sample. We now see that quoting only a single value when characterizing the binding energy as a function of surface coverage, as done in most previous studies<sup>4-6</sup>, is an oversimplification.

The relative distribution of  $E_b$  values varied little among all of our  $H_2/H_2O$  depositions at 12 K, even though the total amount of condensed  $H_2O$  varied by more than an order of magnitude. These results suggest that the observed distribution of  $E_b$  values is characteristic of the bulk ice sample. As noted above, many of the high  $E_b$  sites may be specifically due to deeply buried locations, which would explain the observed disappearance of sites with  $E_b > 1100$  K in very thin (low  $H_2O$ , with total ice thickness  $\leq 100 \text{ \AA}$ ) samples. Our measurements do not appear to support the suggestion<sup>10</sup> that the  $H_2$  released as the sample was heated above  $\sim 35$  K had been physically trapped in the ice, because one would then expect a significant increase in the relative population of high  $E_b$  sites as the sample thickness increased. Rather,  $H_2$  molecules appear to freely migrate in the ice until finding a vacant binding site, as expected for a solid that is microporous throughout the whole volume.

This understanding of the energetics of  $H_2$  binding sites in amorphous  $H_2O$  ice allows us to estimate the  $H_2$  composition of interstellar ice mantles in cold molecular clouds. Since the collision frequency ( $\tau_{col}^{-1}$ ) of hydrogen with

interstellar grains is much faster than that of water, sites for which  $\tau_{\text{sub}} \geq \tau_{\text{col}}$  are always filled by  $\text{H}_2$ . In dark clouds,  $\tau_{\text{col}}(\text{H}_2) \approx 10^6$  sec, taking the number density  $n(\text{H}_2) \sim 10^4 \text{ cm}^{-3}$  and assuming a typical binding site cover  $10^{-15} \text{ cm}^2$ . Then for grain temperatures of 10K, all sites with  $E_b \geq 440\text{K}$  are filled. Since this is the same threshold value for  $E_b$  for 12K ice in our laboratory experiments, given the sampling timescale, we therefore expect the bulk composition of ice mantles that form on interstellar grains in molecular clouds will be close to our laboratory result.

Our laboratory simulation predicts that ice mantles in interstellar dark clouds are composed largely of  $\text{H}_2$ , about twice that of  $\text{H}_2\text{O}$  (even larger in mantles formed at temperatures colder than 10 K). If these grains are then heated even up to  $>40$  K, significant amounts of  $\text{H}_2$  will remain in the icy mantle, with the results shown in figure 3 providing an estimate of the amount remaining. Ice mantles grown at 20 K in warmer interstellar clouds will have a smaller, but still significant,  $\text{H}_2$  abundance ( $\text{H}_2/\text{H}_2\text{O} \leq 0.5$ ), as we expect all sites with  $E_b \geq 875$  K to be filled by  $\text{H}_2$ . Thus the composition of grain mantles should be directly related to their formation and evolutionary history.

Such a large amount of  $\text{H}_2$  that can be present in cold ice mantles may be detectable with current observational capabilities. Laboratory measurements of a feature near  $2.42\mu\text{m}$  ( $4140\text{cm}^{-1}$ ) in the  $\text{H}_2/\text{H}_2\text{O}$  ice, due to induced stretching bands of adsorbed  $\text{H}_2$ , has been reported by others<sup>6, 13</sup>. In our experiments, large abundances of incorporated  $\text{H}_2$  had no noticeable effect on the  $3.1\mu\text{m}$  water ice band, readily detected in interstellar clouds<sup>2</sup>, nor was the  $2.42\mu\text{m}$  feature detected, possibly due to the thinness of our ice samples.

Significant quantities of molecular hydrogen incorporated in the water ice mantles of interstellar grains will clearly affect grain chemistry and physics.  $\text{H}_2$  would fill the most energetic sites on the surface, leaving only low energy sites for the physisorption of other molecules. Heavy chemical species will be bound less strongly to, and desorb more easily from, an  $\text{H}_2$  rich ice surface<sup>3</sup>, predicting less depletion of heavy species onto grains. Atomic and molecular mobility over the surface<sup>14</sup> and through the volume of amorphous ice mantles will be very different if the ice is saturated with  $\text{H}_2$ , with a consequent impact on chemical reaction rates. The abundance of  $\text{H}_2$  in the bulk ice mantle would provide a more reducing environment for energetic reactions in the mantle, such as those occurring in ice irradiation experimental simulations<sup>12, 15, 16</sup>. Lastly, the increase in the ice mantle number density from the bound  $\text{H}_2$  should result in a higher heat capacity of the grain mantle than in previous estimates, thereby changing our understanding of mantle heating processes.

Acknowledgements: This work represents one phase of research carried out at the Jet Propulsion Laboratory, California Institute of Technology, under contract to the National Aeronautics and Space Administration. One of us (RWD) would like to thank the NASA Graduate Student Researchers Program for their support. The comments of G. Blake, W. Langer, and M. Werner are appreciated

1. Tielens, A.G.G.M. in *Interstellar Dust, IAU Symposium 135* (eds. Allamandola, L.J. & Tielens, A.G.G.M.) 239-262 (Kluwer Academic Publishers, Dordrecht, 1989).
2. Whittet, D.C.B., *et al. Mon. Not. R. astr. Soc.* **233**, 321-336 (1988).
3. Allen, M. & Robinson, G.W. *Astrophys. J.* **212**, 396-415 (1977).
4. Govers, T.R., Mattera, L. & Scoles, G. *J. Chem. Phys.* **72**, 5446-5455 (1980).
5. Lee, T.J. *Nature* **237**, 99 (1972).
6. Sandford, S.A. & Allamandola, L.J. (1993, In Press).
7. Hollenbach, D. & Salpeter, E.E. *Astrophys. J.* **163**, 155-164 (1971).
8. d'Hendecourt, L.B., Allamandola, L.J. & Greenberg, J.M. *Astr. Astrophys.* **152**, 130-150 (1985).
9. Tielens, A.G.G.M. & Hagen, W. *Astr. Astrophys.* **114**, 245-260 (1982).
10. Laufer, D., Kochavi, E. & Bar-Nun, A. *Phys. Rev. B* **36**, 9219-9227 (1987).
11. Mayer, E. & Pletzer, R. *Nature* **319**, 298-301 (1986).
12. Allamandola, L.J., Sandford, S.A. & Valero, G.J. *Icarus* **76**, 225-252 (1988).
13. Hixson, H.G., Woycik, M.J., Devlin, M.S., Devlin, J.P. & Buch, V. *J. Chem. Phys.* **97**, 753-767 (1992).
14. Smoluchowski, R. *J. Phys. Chem.* **87**, 4229-4233 (1983).
15. Pirronello, V., Brown, W.L., Lanzerotti, L.J., Marcantonio, K.J. & Simmons, E.H. *Astrophys. J.* **262**, 636-640 (1982).
16. Greenberg, J.M. *Sci. Am.* **250**, 121-135 (1984).

Fig. 1) Correlation between the  $\text{H}_2$  and  $\text{H}_2\text{O}$  compositions of various ice samples, deposited at a 12 K window temperature (controlled to within  $\pm 0.1$  K by a resistive heater at the base of the window). Absolute abundances of both species were determined by heating the ice samples at 2 K/min, and monitoring the resulting chamber gas composition with a mass spectrometer. Results for the mixtures prepared with  $\text{H}_2:\text{H}_2\text{O}$  gaseous inlet pressures between 4:1 to 36:1 are indicated by filled circles, with deposition times of between 20 minutes and 2.5 hours. Relative abundances of  $\text{H}_2/\text{H}_2\text{O} = 1.6$  and  $3.7$  are indicated with dashed lines. The lower value results from an ice sample allowed to sit in the chamber for several hours after deposition while  $\text{H}_2\text{O}$  apparently was cryopumped from other parts of the vacuum chamber onto the sample, and the higher value from an identically deposited sample allowed to sit several hours, but now under an atmosphere of  $10^{-5}$  torr of  $\text{H}_2$  maintained in the chamber. Deposition of pure  $\text{H}_2$  for 1 hour is indicated by an open square, and deposition of pure water for 1 hour by an open triangle. Residual water and hydrogen in the system made repeatability of experimental results difficult, and we suggest that systematic errors caused by this are responsible for the uncertainty in the measurements represented by the scatter of the data.

Fig. 2) Time-varying desorption rates for  $\text{H}_2$  and  $\text{H}_2\text{O}$  as functions of temperature as the ice sample was heated steadily. The inlet gas pressures for  $\text{H}_2$  and  $\text{H}_2\text{O}$  were 0.8 and 0.2 torr, respectively, for a 70 minute deposition. The results of three different experiments are shown, with identical conditions except for the window temperature.  $\text{H}_2$  desorption profiles for window temperatures of 12 K, 20 K, and 30 K are indicated by filled squares, open diamonds, and crosses, respectively. The desorption profile of  $\text{H}_2\text{O}$  from the 12 K deposition is indicated by open squares. Lines between markers serve only to aid visualization, and do not represent actual data. The  $\text{H}_2$  desorption profiles for the 20 K and 30 K depositions were normalized by setting the  $\text{H}_2\text{O}$  abundance from these samples equal to that of the water abundance in the 12 K deposition. The total amounts of  $\text{H}_2$  and  $\text{H}_2\text{O}$  in each sample were found by integrating under such desorption curves.

Fig. 3) Time-varying hydrogen desorption profile (filled circles) for stepwise heating of an  $\text{H}_2/\text{H}_2\text{O}$  ice mixture, prepared as described in figure 2, with a window temperature of 12 K. The dashed line represents the time-dependent heating profile, with the window temperature held constant at 20 K, 30 K, and 40 K, for  $\sim 10$  minutes at each temperature. Again, the line between markers serves only as a visualization aid.

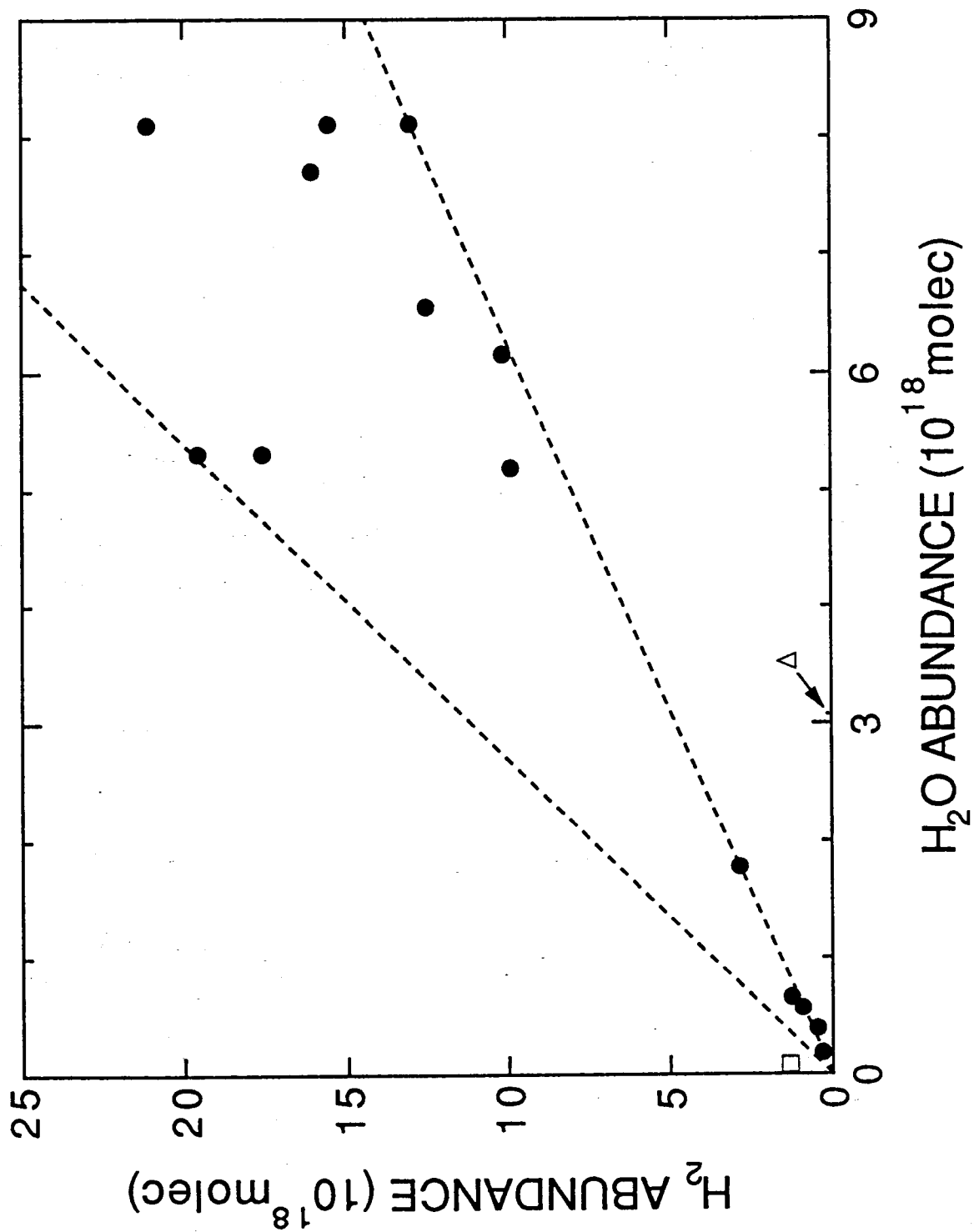


Fig. 1

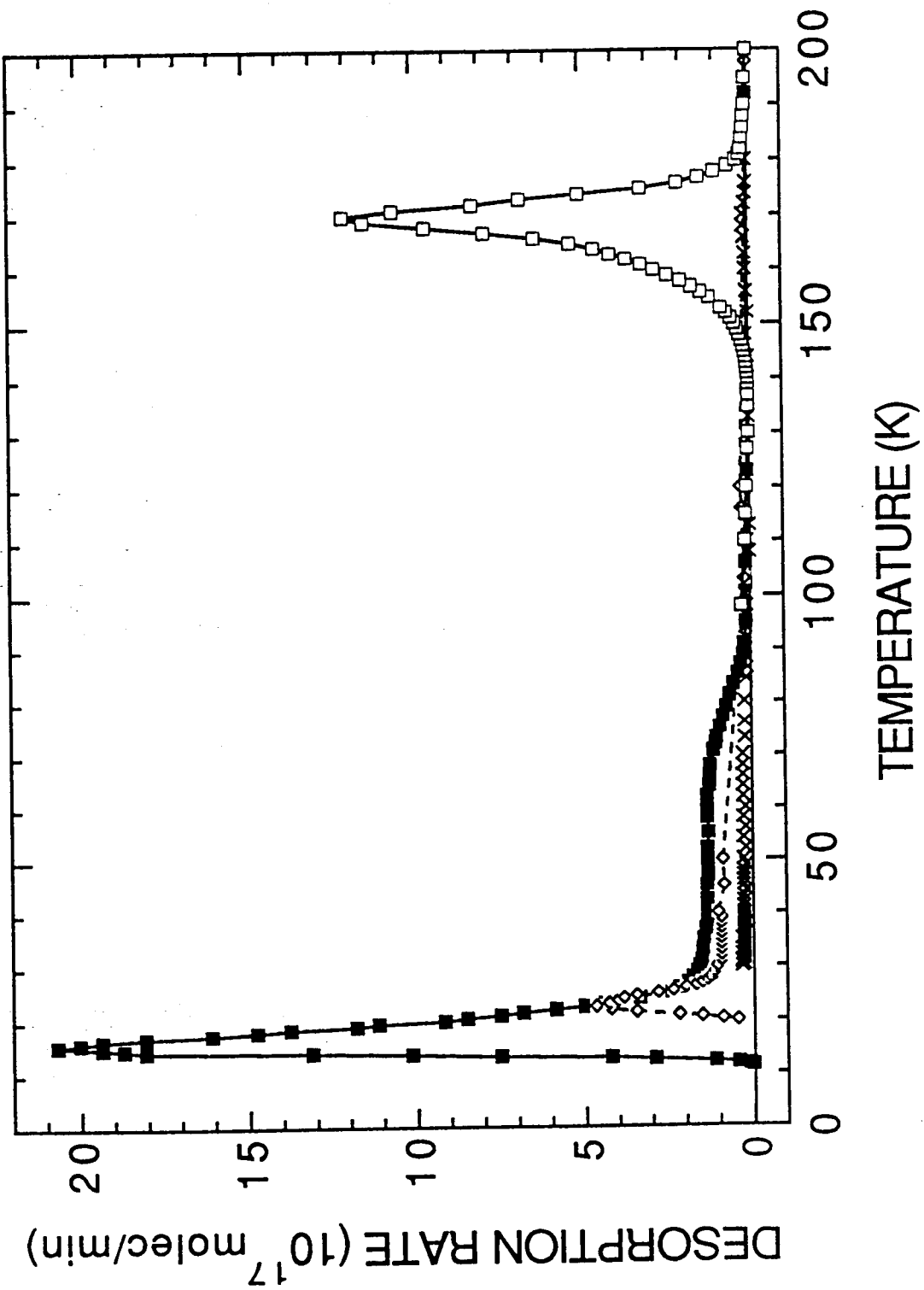


Fig. 2

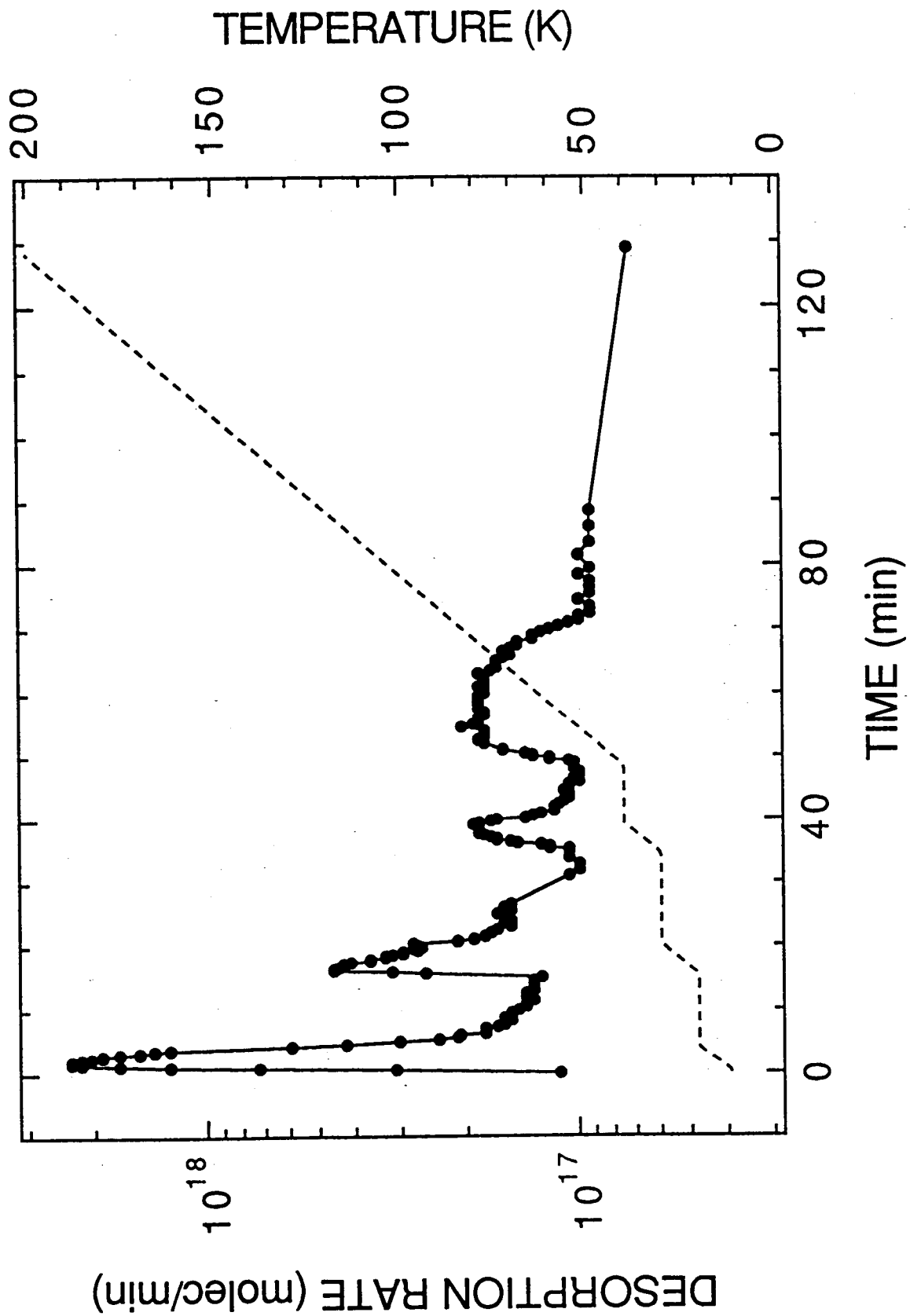


Fig. 3